CURRENT CONTROL WITH 3D SPACE VECTOR MODULATION FOR THREE-PHASE FOUR-WIRE ACTIVE FILTERS

Marcelo Gradella Villalva*, Milton E. de Oliveira Filho† and Ernesto Ruppert Filho‡
School of Electrical and Computer Engineering
Campinas State University (UNICAMP), Campinas, SP, Brazil
* Email: mvillalv@dsce.fee.unicamp.br
† Email: mfilho@dsce.fee.unicamp.br
‡ Email: ruppert@fee.unicamp.br

***Abstract*— This research presents the detailed implementation of a current controller with three-dimension (3D) space vector pulse width modulation (SVPWM) for active filters used in four-wire unbalanced power systems. Many techniques of current control are widely known for three-wire balanced systems. However, some modifications must be done in the original techniques when the system is unbalanced and has a neutral conductor. Few works are explicit and detailed on this subject. This paper shows the complete process of implementation of a four-wire current controller with a three-leg inverter and makes a comparison of its performance with the performance of the conventional hysteresis-based current controller.**

***Keywords*—current control, four-wire active filter, three-leg inverter, space vector**

I. INTRODUCTION

Shunt active filters are used in three-phase systems to compensate harmonic and reactive currents. When they are used in four-wire systems they can also compensate load unbalance. In four-wire systems the neutral current (if it exists) and the line currents must be compensated together.

Figure 1 shows a shunt active power filter scheme for four-wire systems. A three-leg inverter with two-capacitor split dc-link is used instead of a four-leg inverter. Although a four-leg inverter increases the robustness of the control system a three-leg inverter is better due to its simplicity and reduced number of switches. In the scheme presented in figure 1 the neutral of the electric system is connected to the middle point of the dc-link capacitors. The three-leg inverter and the three inductors L_1, L_2 and L_3 act as a current source for the electric system. The current controller controls the switches S_1-S_6 through a closed-loop control which acts in order to inject in the electric system the appropriate compensation currents. The compensation currents may be calculated by several manners. In three-wire systems they can be calculated as seen in [1]–[4]. In four-wire systems they can be calculated as seen in [5]–[7]. In the scheme presented in figure 1 the neutral conductor is connected to the capacitors to allow the flow of zero-sequence currents when the load is unbalanced. These currents must be compensated by the active filter.

A good current control method is essential for the overall performance of the active filter. Many techniques of current control have been developed in the past years. In [8] there is a good overview of many current control techniques. However the referred work treats only of three-wire systems.

Two widely known techniques are the hysteresis-based current control and the proportional-integral current control with pulse width modulation (PWM). The first one is robust, fast and relatively simple. The latter has a lower dynamic response but is very adequate for the implementation in digital systems and has fixed switching frequency. Nevertheless a fixed switching frequency may be obtained with the hysteresis control through some additional complexities. Works like [9]–[11] show how this can be done in three-wire systems. Reference [12] shows an hysteresis-based current controller for four-wire systems.

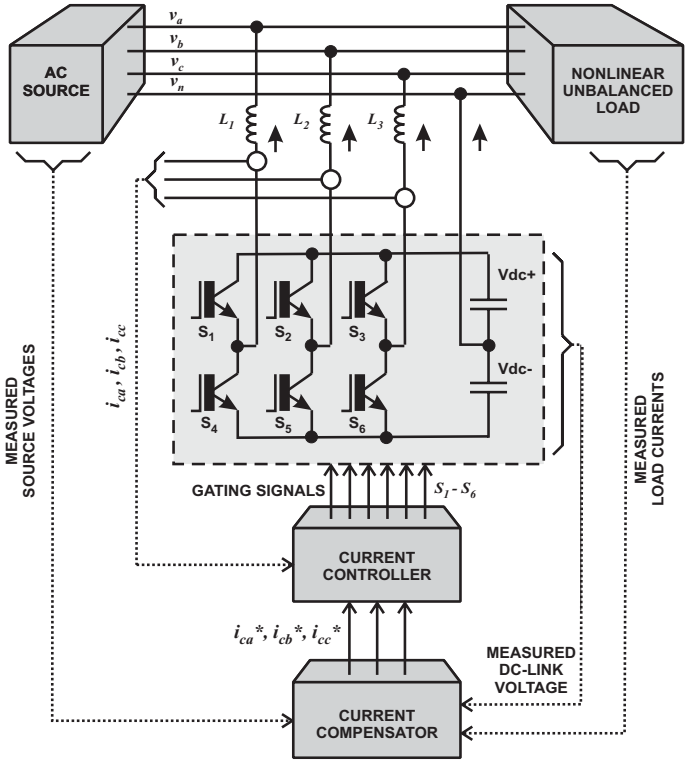

Fig. 1. Shunt active power filter in four-wire system.

II. FOUR-WIRE HYSTERESIS CURRENT CONTROL

This section briefly discusses the hysteresis-based current control technique for four-wire systems presented in [12]. This technique will be used later for a comparison of the performance of the hysteresis-based current control with the performance of the SVPWM-based current control in four-wire systems.

Figure 2 shows the current control scheme presented in [12]. Three comparators with hysteresis are used to compare the reference currents with the measured currents in the $\alpha\beta0$ stationary reference frame. The currents are transformed from the abc three-phase system to the $\alpha\beta0$ system through the $abc \rightarrow \alpha\beta0$ transformation seen in (2).

Figure 3 shows a comparator with hysteresis and its input-output relation. $H = 1$ when $\varepsilon > \delta$ and $H = 0$ when $\varepsilon < -\delta$.

The values of δ_α, δ_β and δ_0 (the comparison thresholds of the three hysteresis comparators of figure 2) are determined in (1),

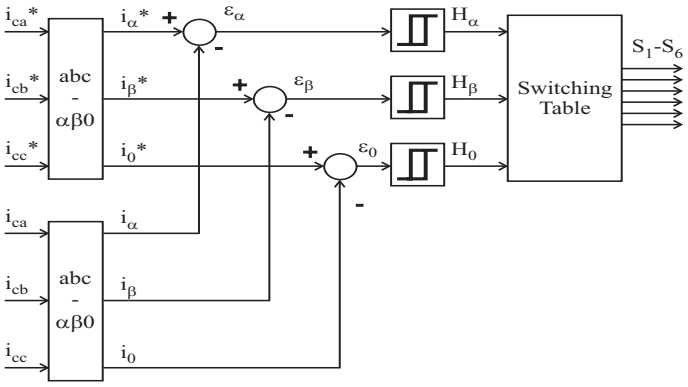

Fig. 2. Hysteresis current control in four-wire system.

TABLE I
SWITCHING TABLE

H_α	0	0	0	0	1	1	1	1
H_β	0	0	1	1	0	0	1	1
H_0	0	1	0	1	0	1	0	1
S_1	1	0	1	0	1	0	1	0
S_2	1	0	0	0	1	1	1	0
S_3	0	0	1	0	1	0	1	1

where δ is a constant which specifies the width of the hysteresis bands.

$$\delta_\alpha = \frac{\sqrt{2}}{\sqrt{3}}\,\delta\ ,\ \delta_\beta = \frac{\sqrt{2}}{3}\,\delta\ ,\ \delta_0 = \frac{1}{\sqrt{3}}\,\delta \qquad (1)$$

Table I shows the gating signals for the power inverter switches associated with the results of the comparisons. This switching table is found in [12]. By using this table the switches of the power inverter are turned on or off according to the magnitude of the measured currents. If a measured current is greater than a reference current the state of the inverter switches must be changed in order to decrease this measured current. If a measured current is lower than its correspondent reference current another gating pattern must be produced in order to increase it.

This kind of current controller can keep the currents synthesized in the coupling inductors (controlled currents) within an hysteresis band, thus following the reference currents as seen in figure 4.

Although very simple and robust this current control technique has an inherently variable switching frequency because the on and off times of the power inverter switches may have any duration and vary according to the outputs of the hysteresis comparators.

III. THREE-WIRE SVPWM CURRENT CONTROL

Figure 5 shows a current control scheme with pulse width modulation for three-wire systems. A proportional-integral (PI) regulator is used together with a pulse width modulator. The PI regulator minimizes the error signals ε_α and ε_β and provides reference voltages for the modulator. The modulator synthesizes

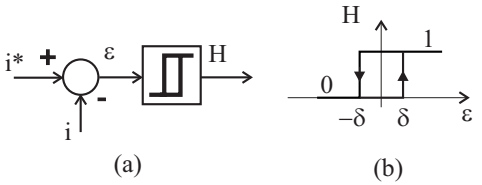

Fig. 3. (a) Comparator with hysteresis. (b) Input-output relation.

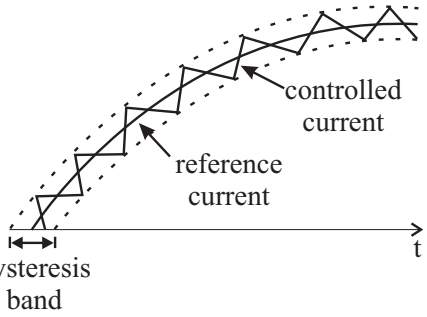

Fig. 4. Reference current and hysteresis-controlled current.

the desired voltages at the output of the power inverter. The power inverter feeds the coupling inductors and synthesizes the active filter currents.

There are many pulse width modulation (PWM) techniques that can be used with this current control method. Reference [13] shows results of some implementations of current controllers with some of the available PWM methods. In [14] the space vector PWM (SVPWM) technique was introduced. This technique provides low harmonic content, improves the utilization of the dc-link voltage, reduces switching losses of the power semiconductors and is very easy to be implemented in digital signal processors.

The current control with the SVPWM technique provides constant switching frequency because the pulse width modulation is done with constant modulation frequency. And the characteristics of the SVPWM technique tend to decrease the amount of high order harmonics at the controlled currents.

IV. FOUR-WIRE SVPWM CURRENT CONTROL

In four-wire systems the current controller must control the active filter line currents (positive and negative sequences) and also the neutral current (zero sequence). In figure 6 there are three reference currents i^*_α , i^*_β and i^*_0 which comprise positive, negative and zero sequence currents of the three-phase system. Three error signals ε_α , ε_β and ε_0 are calculated from the reference currents and from the measured currents i_α , i_β and i_0. The PI controllers receive the error signals and send appropriate signals to the SVPWM inverter. In this case a three-dimension (3D) SVPWM method must be used because the zero sequence current must be controlled. The zero axis is necessary and the original SVPWM technique [14] must be modified [15].

Three-phase abc currents and voltages must be transformed into the $\alpha\beta 0$ space. The $abc - \alpha\beta 0$ transformation is shown in (2).

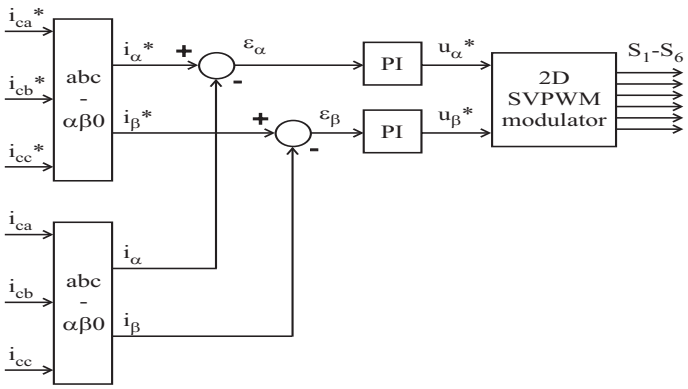

Fig. 5. Three-wire SVPWM current control.

$$\begin{bmatrix} i_\alpha \\ i_\beta \\ i_0 \end{bmatrix} = \sqrt{\frac{2}{3}} \cdot \begin{bmatrix} 1 & -\frac{1}{2} & -\frac{1}{2} \\ 0 & \frac{\sqrt{3}}{2} & -\frac{\sqrt{3}}{2} \\ \frac{1}{\sqrt{2}} & \frac{1}{\sqrt{2}} & \frac{1}{\sqrt{2}} \end{bmatrix} \cdot \begin{bmatrix} i_a \\ i_b \\ i_c \end{bmatrix} \quad (2)$$

A. Electrical system modelling

As seen in [12], the set of power switches of figure 1 may assume eight possible states according to the possible combinations of the six switches. If S_1, S_2 and S_3 are variables that can assume the values 1 (on state) and 0 (off state), the three-phase voltages may be written as follows in (3).

$$\begin{aligned} v_a &= S_1 \cdot V_{dc}^+ - (1 - S_1) \cdot V_{dc}^- \\ v_b &= S_2 \cdot V_{dc}^+ - (1 - S_2) \cdot V_{dc}^- \\ v_c &= S_3 \cdot V_{dc}^+ - (1 - S_3) \cdot V_{dc}^- \end{aligned} \quad (3)$$

Considering that $V_{dc}^+ = V_{dc}^- = V_{dc}/2$ and applying (2) to (3) the $\alpha\beta 0$ voltages seen in table II are found - the voltages are normalized with reference to V_{dc}. Each of the eight possibilities corresponds to a vector in the $\alpha\beta 0$ space. (See figure 8a.)

B. Voltage synthesis

Vectors $\overrightarrow{V_0}$ to $\overrightarrow{V_7}$ seen in table II are used to synthesize voltages in the outputs of the SVPWM-driven inverter according to the desired reference vector $\overrightarrow{V_{ref}}$.

1) Conventional 2D SVPWM: In the original technique [14] the space vectors, which are different of those seen in table II, are located in the $\alpha\beta$ plane - see figure 7. Vectors $\overrightarrow{V_0}$ and $\overrightarrow{V_7}$ are null and cause null voltages in the inverter outputs. The reference voltage $\overrightarrow{V_{ref}}$ is synthesized during small discrete intervals T_{pwm} (modulation period) when two adjacent vectors are used to produce an average output vector. Each adjacent vector remains active during a small fraction of the modulation period T_{pwm}.

The $\overrightarrow{V_{ref}}$ voltage is obtained from (4) and (5). Figure 7 shows this.

$$T_{pwm} \cdot \overrightarrow{V_{ref}} = T_1 \cdot \overrightarrow{V_1} + T_2 \cdot \overrightarrow{V_2} + T_0 \cdot \overrightarrow{V_0} + T_7 \cdot \overrightarrow{V_7} \quad (4)$$

$$\overrightarrow{V_{ref}} = \frac{T_1}{T_{pwm}} \cdot \overrightarrow{V_1} + \frac{T_2}{T_{pwm}} \cdot \overrightarrow{V_2} + \frac{T_0}{T_{pwm}} \cdot \overrightarrow{V_0} + \frac{T_7}{T_{pwm}} \cdot \overrightarrow{V_7} \quad (5)$$

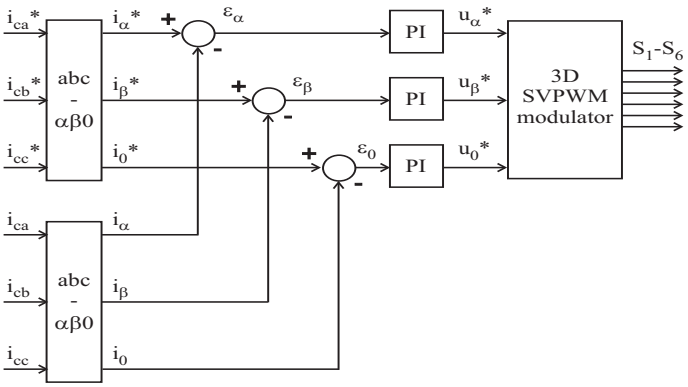

Fig. 6. PI current control in four-wire system.

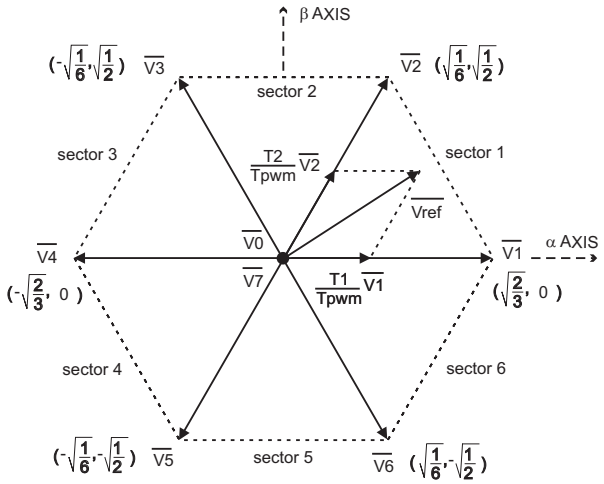

Fig. 7. Vectors in the $\alpha\beta$ plane, conventional SVPWM.

2) 3D SVPWM: In the modified 3D SVPWM technique vectors $\overrightarrow{V_0}$ to $\overrightarrow{V_7}$ are located in the $\alpha\beta 0$ space. The conventional SVPWM strategy may be used if, instead of the conventional $\alpha\beta$ vectors, the projections of the 3D vectors into the $\alpha\beta$ plane are used - see figure 8b. This makes the time intervals of application of null voltages be different of those used in the conventional technique for the synthesis of $\overrightarrow{V_{ref}}$.

Sector identification

Both original and modified SVPWM techniques require the identification of the sector of the $\alpha\beta$ plane the reference vector $\overrightarrow{V_{ref}}$ belongs to. This can be done with the following algorithm:

$$v_{ref}^a = v_\beta$$
$$v_{ref}^b = \frac{\sqrt{3}}{2} \cdot v_\alpha - \frac{1}{2} \cdot v_\beta \quad (6)$$
$$v_{ref}^c = -\frac{\sqrt{3}}{2} \cdot v_\alpha - \frac{1}{2} \cdot v_\beta$$

$$X = \begin{cases} 1 & , v_{ref}^a > 0 \\ 0 & , v_{ref}^a \leq 0 \end{cases} \quad (7)$$

$$Y = \begin{cases} 1 & , v_{ref}^b > 0 \\ 0 & , v_{ref}^b \leq 0 \end{cases} \quad (8)$$

$$Z = \begin{cases} 1 & , v_{ref}^c > 0 \\ 0 & , v_{ref}^c \leq 0 \end{cases} \quad (9)$$

$$N = X + 2Y + 4Z \quad (10)$$

Table III gives the sector in function of N.

TABLE II
VOLTAGES $\alpha\beta 0$ AS FUNCTIONS OF S1, S2 AND S3

S_1	0	1	1	0	0	0	1	1
S_2	0	0	1	1	1	0	0	1
S_3	0	0	0	0	1	1	1	1
v_a	$-\frac{1}{2}$	$\frac{1}{2}$	$\frac{1}{2}$	$-\frac{1}{2}$	$-\frac{1}{2}$	$-\frac{1}{2}$	$\frac{1}{2}$	$\frac{1}{2}$
v_b	$-\frac{1}{2}$	$-\frac{1}{2}$	$\frac{1}{2}$	$\frac{1}{2}$	$\frac{1}{2}$	$-\frac{1}{2}$	$-\frac{1}{2}$	$\frac{1}{2}$
v_c	$-\frac{1}{2}$	$-\frac{1}{2}$	$-\frac{1}{2}$	$-\frac{1}{2}$	$\frac{1}{2}$	$\frac{1}{2}$	$\frac{1}{2}$	$\frac{1}{2}$
v_α	0	$\sqrt{\frac{2}{3}}$	$\frac{1}{\sqrt{6}}$	$-\frac{1}{\sqrt{6}}$	$-\sqrt{\frac{2}{3}}$	$-\frac{1}{\sqrt{6}}$	$\frac{1}{\sqrt{6}}$	0
v_β	0	0	$\frac{1}{\sqrt{2}}$	$-\frac{1}{\sqrt{2}}$	0	$-\frac{1}{\sqrt{2}}$	$-\frac{1}{\sqrt{2}}$	0
v_0	$-\frac{\sqrt{3}}{2}$	$-\frac{1}{2\sqrt{3}}$	$\frac{1}{2\sqrt{3}}$	$-\frac{1}{2\sqrt{3}}$	$\frac{1}{2\sqrt{3}}$	$-\frac{1}{2\sqrt{3}}$	$\frac{1}{2\sqrt{3}}$	$\frac{\sqrt{3}}{2}$
	$\overrightarrow{V_0}$	$\overrightarrow{V_1}$	$\overrightarrow{V_2}$	$\overrightarrow{V_3}$	$\overrightarrow{V_4}$	$\overrightarrow{V_5}$	$\overrightarrow{V_6}$	$\overrightarrow{V_7}$

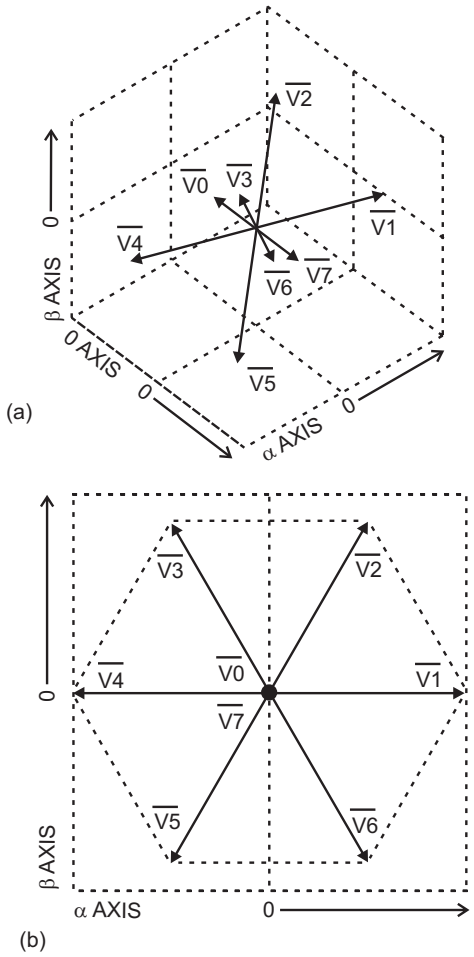

Fig. 8. (a) Vectors in the $\alpha\beta 0$ space, 3D SVPWM. (b) Projections into the $\alpha\beta$ plane.

Determination of the time intervals

Next step is to obtain the time intervals T_1 and T_2 (for sector 1), T_2 and T_3 (for sector 2), T_3 and T_4 (for sector 3), T_4 and T_5 (for sector 4), T_5 and T_6 (for sector 5), T_6 e T_1 (for sector 6). These time intervals must be separately calculated for each sector by the expressions (13) through (18). These expressions are obtained from (11) and (12). The vectors of (11) are those of table II.

$$\vec{V_k} = V_k^{\alpha} \cdot \hat{\alpha} + V_k^{\beta} \cdot \hat{\beta} + V_k^{0} \cdot \hat{0} \ , \quad k \ \epsilon \ \{1, \cdots, 6\} \tag{11}$$

$$\begin{bmatrix} T_k \\ T_{k+1} \end{bmatrix} = T_{pwm} \cdot \begin{bmatrix} V_k^{\alpha} & V_{k+1}^{\alpha} \\ V_k^{\beta} & V_{k+1}^{\beta} \end{bmatrix}^{-1} \cdot \begin{bmatrix} v_{\alpha} \\ v_{\beta} \end{bmatrix} \tag{12}$$

$$\begin{bmatrix} T_1 \\ T_2 \end{bmatrix} = T_{pwm} \cdot \begin{bmatrix} 1/2\sqrt{6} & -1/2\sqrt{2} \\ 0 & \sqrt{2} \end{bmatrix} \cdot \begin{bmatrix} v_{\alpha} \\ v_{\beta} \end{bmatrix} \tag{13}$$

$$\begin{bmatrix} T_2 \\ T_3 \end{bmatrix} = T_{pwm} \cdot \begin{bmatrix} 1/2\sqrt{6} & 1/2\sqrt{2} \\ -1/2\sqrt{6} & 1/2\sqrt{2} \end{bmatrix} \cdot \begin{bmatrix} v_{\alpha} \\ v_{\beta} \end{bmatrix} \tag{14}$$

TABLE III
SECTOR IDENTIFICATION.

N	1	2	3	4	5	6
Sector	2	6	1	4	3	5

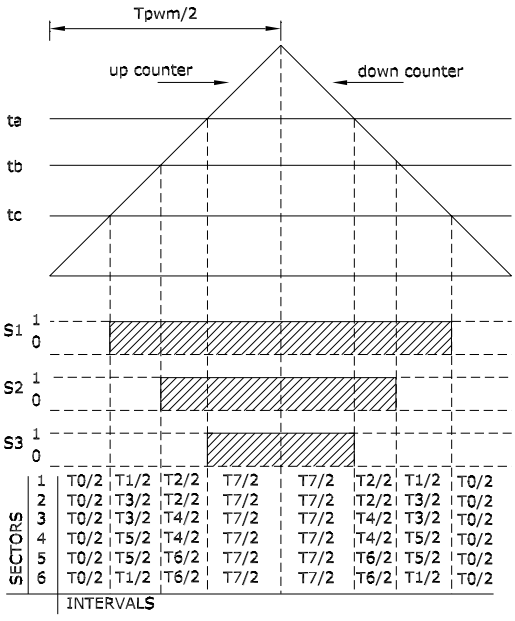

Fig. 9. Generation of the the SVPWM pulses.

$$\begin{bmatrix} T_3 \\ T_4 \end{bmatrix} = T_{pwm} \cdot \begin{bmatrix} 0 & \sqrt{2} \\ -1/2\sqrt{6} & -1/2\sqrt{2} \end{bmatrix} \cdot \begin{bmatrix} v_{\alpha} \\ v_{\beta} \end{bmatrix} \tag{15}$$

$$\begin{bmatrix} T_4 \\ T_5 \end{bmatrix} = T_{pwm} \cdot \begin{bmatrix} -1/2\sqrt{6} & 1/2\sqrt{2} \\ 0 & -\sqrt{2} \end{bmatrix} \cdot \begin{bmatrix} v_{\alpha} \\ v_{\beta} \end{bmatrix} \tag{16}$$

$$\begin{bmatrix} T_5 \\ T_6 \end{bmatrix} = T_{pwm} \cdot \begin{bmatrix} -1/2\sqrt{6} & -1/2\sqrt{2} \\ 1/2\sqrt{6} & -1/2\sqrt{2} \end{bmatrix} \cdot \begin{bmatrix} v_{\alpha} \\ v_{\beta} \end{bmatrix} \tag{17}$$

$$\begin{bmatrix} T_6 \\ T_1 \end{bmatrix} = T_{pwm} \cdot \begin{bmatrix} 0 & -\sqrt{2} \\ 1/2\sqrt{6} & 1/2\sqrt{2} \end{bmatrix} \cdot \begin{bmatrix} v_{\alpha} \\ v_{\beta} \end{bmatrix} \tag{18}$$

The time intervals of the 0 axis vectors are calculated by (19) and (20).

$$T_7 = v_0\, T_{pwm}/\sqrt{3} - 2T_2/3 - T_1/3 + T_{pwm}/2 \tag{19}$$

$$T_0 = T_{pwm} - T_2 - T_1 - T_7 \tag{20}$$

Generation of the switching pulses

The generation of the six pulses for the inverter switches can be done by three digital comparators and an up-down counter. Most digital signal processors provide this facility. Generally there are at least three comparators and at least one up-down counter that allow the easy implementation of the 3D SVPWM technique.

Figure 9 shows the process of pulse generation. Each of the three comparison values (t_a,t_b,t_c) correspond to one of the three upper switches of the power inverter. If the reference vector is in sector 1, S_1 (figure 1) must be on only when the counting is greater than the comparison level t_a. By analogy, S_2 must be on

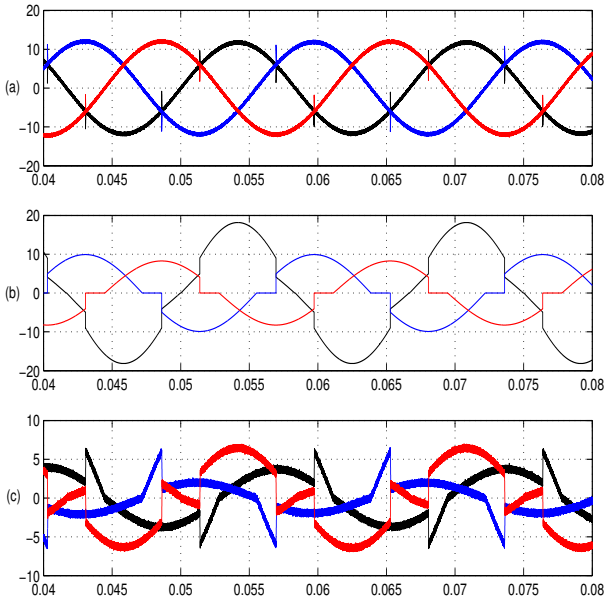

Fig. 10. (a) Source compensated currents, (b) load currents, (c) compensation currents. Units are *ampères* and *seconds*.

when the counting is greater than the level t_b and S_3 is on when the counting is greater than t_c. The levels t_a, t_b and t_c depend on the sector $\overrightarrow{V_{ref}}$ is in and are calculated from the time intervals T_0 through T_7 according to tables IV, V and VI.

V. Results

An active filter for a four-wire system (figure 1) was simulated with the SimPowerSystems blockset of Matlab/Simulink. In the simulation the nonlinear load of figure 14 was connected to the sinusoidal three-phase source. The highly nonlinear load currents where compensated with an active filtering scheme like that of figure 1. The studied current control method with the neutral conductor connected to the middle point of the capacitors and using the 3D SVPWM technique made possible the correct compensation of the harmonic, reactive and zero sequence currents. This simulation used $V_f = 100V_p$, $f = 60Hz$, $L1 = L2 = L3 = 2mH$, $V_{dc}^{+} = V_{dc}^{-} = V_{dc}/2 = 200V$ and $T_{pwm} = 100\mu s$. The PI regulators were adjusted with $kp = 5$ and $ki = 0.2$. Figure 10

TABLE IV

Determination of t_a

Setor	t_a
1	$T_0/2$
2	$T_0/2 + T_3/2$
3	$T_0/2 + T_3/2 + T_4/2$
4	$T_0/2 + T_4/2 + T_5/2$
5	$T_0/2 + T_5/2$
6	$T_0/2$

TABLE V

Determination of t_b

Setor	t_b
1	$T_0/2 + T_1/2$
2	$T_0/2$
3	$T_0/2$
4	$T_0/2 + T_5/2$
5	$T_0/2 + T_5/2 + T_6/2$
6	$T_0/2 + T_6/2 + T_1/2$

TABLE VI

Determination of t_c

Setor	t_c
1	$T_0/2 + T_1/2 + T_2/2$
2	$T_0/2 + T_2/2 + T_3/2$
3	$T_0/2 + T_3/2$
4	$T_0/2$
5	$T_0/2$
6	$T_0/2 + T_1/2$

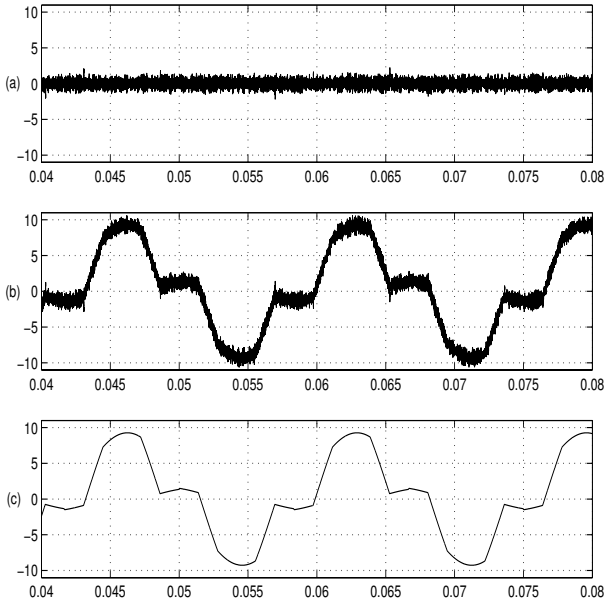

Fig. 11. (a) Neutral current of the source, (b) neutral current of the active filter, (c) neutral current of the load. Units are *ampères* and *seconds*.

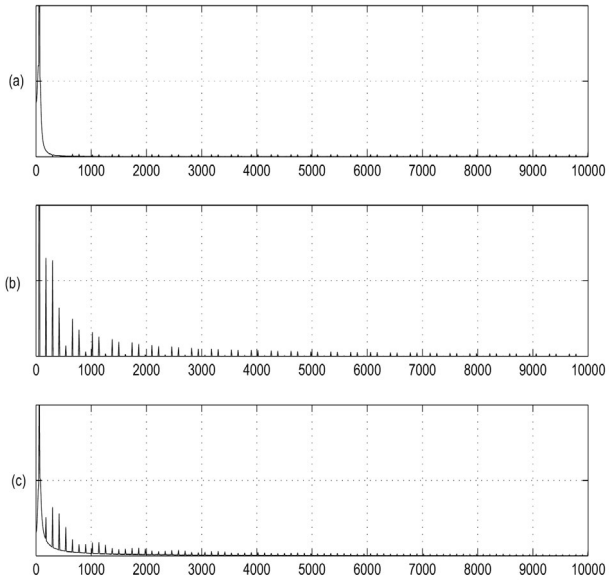

Fig. 12. Frequency spectra of the currents with the studied method. (a) Source current, (b) load current, (c) compensation current. Frequencies are in $hertz$.

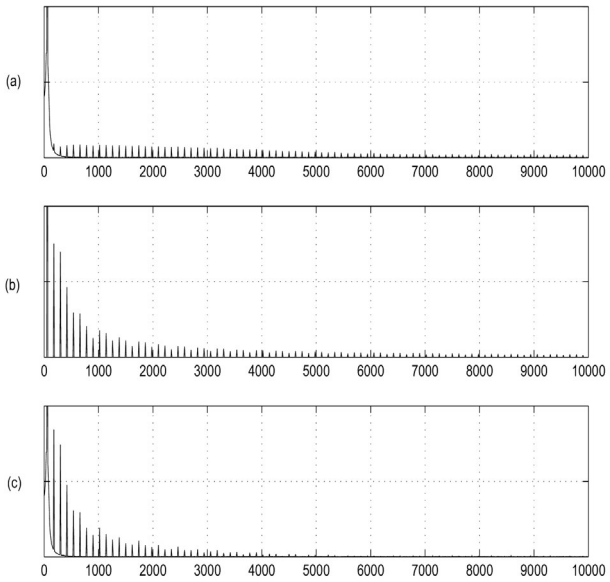

Fig. 13. Frequency spectra of the currents with the hysteresis-based control method. (a) Source current, (b) load current, (c) compensation current. Frequencies are in $hertz$.

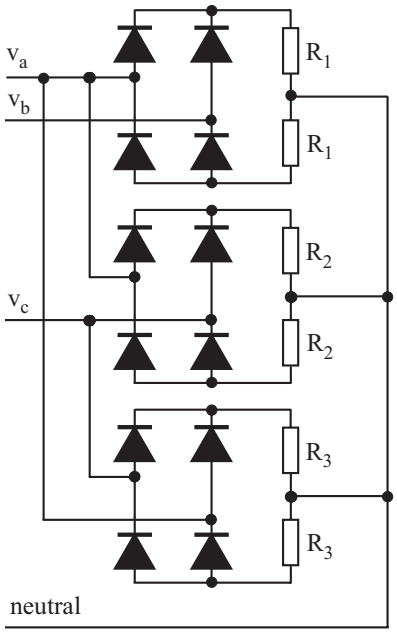

Fig. 14. Nonlinear load used in the simulation.

shows the compensated currents of the ac source, the load currents and the compensation currents injected in the system by the active filter, in this sequence. Figure 11 shows the neutral currents of the source, of the active filter and of the load.

The frequency spectra of the phase a currents are shown in figure 12. In order to verify the performance of the studied control strategy it was compared with the hysteresis-based technique for four-wire systems [12]. Figure 13 shows the frequency spectra of the phase a currents when the hysteresis current control is used.

VI. Conclusion

This research has presented the detailed process of implementation of a current controller with 3D SVPWM for active filters in three-phase four-wire systems. A simulation of an active filter used with an unbalanced system has validated the studied current control method.

A comparison with the hysteresis-based control [12] has shown that the studied method has a better performance. This method allows the compensation of positive, negative and zero sequence currents and its performance is excellent, as seen in figure 12.

The next step of this research is to implement laboratory prototypes of this and other types of current controllers.

Acknowledgement

The authors are grateful to FAPESP - Fundação de Amparo à Pesquisa do Estado de São Paulo - for the financial support.

References

[1] Shin-Kuan Chen and Gary W. Chang. A new instantaneous power theory-based three-phase active power filter. *Proceedings of the IEEE Power Engineering Society Winter Meeting*, 4, 2000.

[2] Edson H. Watanabe and Mauricio Aredes. Compensation of non-periodic currents using the instantaneous power theory. *Proceedings of the IEEE Power Engineering Society Summer Meeting*, 2:994–999, July 2000.

[3] Hirofumi Akagi, Yoshihira Kanazawa, and Akira Nabae. Instantaneous reactive power compensators comprising switching devices without energy storage components. *IEEE Transactions on Industry Applications*, IA-20(3):625–630, 1984.

[4] Hirofumi Akagi, Akira Nabae, and Satoshi Atoh. Control strategy of active power filters using multiple voltage-source pwm converters. *IEEE Transactions on Industry Appplications*, IA-22(3):460–465, 1986.

[5] Hirofumi Akagi, Satoshi Ogasawara, and Hyosung Kim. The theory of instantaneous power in three-phase four-wire systems: A comprehensive approach. *Proceedings of the IEEE Industry Applications Conference*, 1:431–439, October 1999.

[6] Mauricio Aredes and Edson H. Watanabe. New control algorithms for series and shunt three-phase four-wire active power filters. *IEEE Transactions on Power Delivery*, 10(3):1649–1656, July 1995.

[7] Mauricio Aredes, J. Hafner, and Klemens Heumann. Three-phase four-wire shunt active filter control strategies. *IEEE Transactions on Power Electronics*, 12(2):311–318, March 1997.

[8] S. Buso, L. Malesani, and P. Mattavelli. Comparison of current control techniques for active filter applications. *IEEE Transactions on Industrial Electronics*, 45(5):722–729, October 1998.

[9] Ching-Tsai Pan and Ting-Yu Chang. An improved hysteresis current controller for reducing switching frequency. *IEEE Transactions on Power Electronics*, 9(1):97–104, January 1994.

[10] Luigi Malesani and Paolo Tenti. A novel hysteresis control method for current-controlled voltage-source pwm inverters with constant modulation frequency. *IEEE Transactions on Industry Applications*, 26(1):88–92, Januray/February 1990.

[11] D. Wuest and F. Jenni. Space vector based current control schemes for voltage source inverters. *Proceedings of the 24th Annual IEEE Power Electronics Specialists Conference, PESC '93*, pages 986–992, June 1993.

[12] Pedro Verdelho and G. D. Marques. Four-wire current-regulated pwm voltage converter. *IEEE Transactions on Industrial Electronics*, 45(5):761–770, October 1998.

[13] J. W. Dixon, S. Tepper, and L. Morán T. Analysis and evaluation of different modulation techniques for active power filters. *Proceedings of the 9th Annual IEEE Applied Power Electronics Conference and Exposition, APEC '94*, 2:894–900, February 1994.

[14] H. W. van der Broeck, Hans-Christoph Skudelny, and G. Viktor Stanke. Analysis and realization of a pulsewidth modulator based on voltage space vectors. *IEEE Transactions on Industry Applications*, 24(1):140–150, January/February 1988.

[15] Changjiang Zhan, A. Arulampalam, V. K. Ramachandaramurthy, C. Fitzer, M. Barnes, and N. Jenkins. Novel voltage space vector pwm algorithm of 3-phase 4-wire power conditioner. *Proceedings of the IEEE Power Engineering Society Winter Meeting*, 3:1045–1050, February 2001.